Eur Biophys J (1989) 17:87–100

European Biophysics Journal

The influence of structural variations in the F- and FG-helix of the β-subunit modified oxyHb-NES on the heme structure detected by resonance Raman spectroscopy

R. Schweitzer-Stenner, D. Wedekind, and W. Dreybrodt

Fachbereich 1 – Institut für Physik, Universität Bremen, D-2800 Bremen, Federal Republic of Germany

Received July 7, 1988/Accepted in revised form January 9, 1989

Abstract. The dispersion of the depolarization ratio of two prominent Raman lines (1,375 cm^{-1} and 1,638 cm^{-1}) of oxyhemoglobin-N-ethyl succinimide have been examined for pH values between pH = 6.0 and 8.5. Both exhibit a significant pH dependence. Calculation of the Raman tensor in terms of a fifth-order time dependent theory provides information about the pH-dependence of parameters reflecting symmetry classified distortions of the prosthetic heme group. To correlate these distortions with the functional properties of the molecule the following protocol was used: *1)* An allosteric model suggested by Herzfeld and Stanley (1974) has been applied to O_2-binding curves measured at different pH values between 6.5 and 9.0. From this calculation one obtains both, the energy differences between different molecular conformations and the equilibrium constants of oxygen and proton binding. *2)* A titration model was formulated relating each conformation of a molecule to a distinct set of distortion parameters of the heme group. *3)* The distortion parameters resulting from the analysis of our Raman data were assigned as an effective value due to incoherent superposition of the distortion parameters related to the different titration states. The application of this procedure yields an excellent reproduction of the pH-dependent effective distortion parameters of both Raman lines investigated. It is shown that the protonation of two tertiary effector groups located in the β-subunits affect the symmetry of the heme in a contrary manner: the protonation of a His-residue (pK = 8.2, probably His(FG4)β) causes a symmetric position of the proximal imidazole thus lowering the perturbations of the heme core. Further it influences the interaction between amino acid residues of the heme cavity and pyrrole side chains (probably Val(FG5)β-vinyl (pyrrole 3) thus causing a decrease of the distortions related to the peripheral part of the heme. In contrast, the protonation of Lys(EF6)β causes a tilt position of the proximal imidazole and an increase of asymmetric perturbations of the heme core, whereas the interaction between the pyrrole side chains and the heme cavity is weakened. Our results are consistent with stereochemical predictions of Moffat (1971) concerning the existence of an H-bond between His(FG4)β and Cys(F9)β.

Key words: Oxyhemoglobin-NES, resonance Raman scattering, depolarization ratio, tertiary effector binding, Bohr effect, heme-apoprotein interactions

Introduction

The relationship between functional properties of heme-proteins (i.e. binding affinity for different ligands such as O_2, CO, NO and heterotropic interactions between ligand and ion binding sites (H^+, Cl^-)) and associated variations of the tertiary and quaternary structures is one of the main objectives of investigations dealing with these biological systems. In this context one aims to get detailed knowledge of the coupling mechanisms, which are involved in the transduction of structural changes from the protein to the functional heme group via distinct pathways.

As we have shown in a previous paper (Schweitzer-Stenner and Dreybrodt 1985), resonance Raman scattering can be applied in order to detect distortions of the heme group from its ideal D_{4h}-symmetry, which are due to heme-apoprotein interactions. This has been achieved by measuring the depolarization ration dispersion (DPR) and the corresponding excitation profiles (EPs) of structurally sensitive Raman lines. By a subsequent thorough analysis in terms of a fifth-order time-dependent perturbation theory (Loudon 1973), this procedure provides distortion parameters which are, to a first approximation, linearly related to

Abbreviations: DPR: depolarization ratio; EP: excitation profile; HbA: human hemoglobin; oxyHb: oxyhemoglobin; NEM: N-ethyl-maleimide; NES: N-ethyl-succimide; BME: Bis(N-maleimidodimethyl)ether.

the amplitude of symmetry classified normal distortions δQ^{Γ} of the prosthetic group ($\Gamma = A_{1g}$, B_{1g}, B_{2g}, and A_{2g} representations in D_{4h}-symmetry). The applicability of this method has recently been demonstrated by Schweitzer-Stenner et al. (1986) and Brunzel et al. (1986) in the following way: They measured the pH-dependence of the DPR-dispersion of two prominent oxyHb-Raman lines (1,375 cm^{-1} and 1,638 cm^{-1}) at low Cl^- ion concentrations. The analysis of the data yielded a pH-dependence of the heme perturbations. This pH-dependence has been explained by the following model. Protonation processes of several titrable amino acid groups of the protein, change its environment. This conformational change is transduced to the heme groups thus effecting distortions specific to each titration state. Thus the measured Raman intensities result from incoherent superposition of several distinct kinds of porphyrin molecules. The pH-dependence of the Raman data is provided by the variation of the occupation numbers of the titrable groups involved upon changing the pH value of the solution.

Applying this model to oxyHb, three titrable groups with pK = 5.8, 6.6 and 7.8 were found. In order to test the validity of this result, similar titration models have been applied to data reflecting the pH-dependence of the optical absorption (Brunzel et al. 1986) and of the kinetic constants related to the fourth binding step of oxygen and carbon monoxide binding to HbA (deYoung et al. 1976; Kwiatkowski and Noble 1982). Excellent agreement in terms of the pK values determined has been obtained. This provides evidence that both the pH-dependence of the heme structure, detected by resonance Raman and optical experiments, and the associated variation in ligand binding have the same origin.

The structural nature of this correlation emerges from the analysis of results obtained from kinetic experiments on modified hemoglobin A (i.e. des(HisHC1)β-Hb and des(HisHC1)β-des(TyrHC2)β-Hb). It shows that the protonation of histidine residues (pK = 6.6) influences the equilibrium between two conformations of the Tyr(HC2)β ring, the existence of which has been reported by Shaanan (1983). At alkaline pH values (pH < 7.0) the Tyr(HC2)β-ring is in a oxy-like position which correlates with an external position of the SH-group of Cys(F9)β. Below pH = 7.0, however, the Tyr(HC2)β-ring occupies, at least partially, a more deoxy like position which results in an internal position of the SH-group of Cys(F9)β. The pH-induced conformational transition from the oxy-like to the deoxy-like Tyr(HC2)β position causes asymmetric heme perturbations and thus results in an increase of the dissociation constant (c.f. Schweitzer-Stenner et al. 1986, Kwiatkowski and Noble 1983).

This interpretation is consistent with the fact that modified oxyHb-BME does not exhibit significant pH-dependence of its heme structure (Brunzel et al. 1986; Wedekind et al. 1985; Wedekind et al. 1986). In this molecule, cooperativity and Bohr effect are absent because of covalent cross linking between His(FG4)β and Cys(F9)β by Bis(N-maleimidomethyl)ether (Perutz 1969; Moffat 1971), which imposes a molecular strain upon the FG-helix of the β-subunit. This most probably blocks the transduction of the conformational change of the Tyr(HC2)β-ring to the chromophore by fixing the position of the SH-group of Cys(F9)β.

To obtain details about this mechanism and to confirm the relationship between structural and functional properties of oxyHb, we have applied this method of resonance Raman investigation to modified oxyHb-NES. In this molecule the sulfhydryl group of Cys(F9)β has been reacted with N-ethyl-maleimide (NEM) to give N-ethyl-succimide (Shih et al. 1984). In contrast to BME, NEM does not crosslink parts of the FG- and F-helix. NEM-treated HbA has increased oxygen affinity, lower cooperativity and a Bohr effect that is half that of HbA (Simon et al. 1971; Kilmartin et al. 1980; Shih et al. 1984). The Hill coefficient depends slighty on the pH value. In order to establish the correlation between heme perturbation and ligand binding for this molecule we have employed the following protocol: First, we measured the DPR-dispersion and the corresponding EPs of the 1,375 cm^{-1} and the 1,638 cm^{-1} fundamentals at different pH values between 6.0 and 8.5, thus covering the region of the alkaline Bohr effect. Second, we extracted the pH-dependence of the heme distortions from these experimental data. Third, we applied the allosteric model suggested by Hertfeld and Stanley (1974) to the oxygen binding curves of HbA-NES which have been reported by Shih et al. (1984). From this we obtained the equilibrium constants for the transitions between different conformational states and for the binding of oxygen and protons to the distinct subunits. Fourth, we constructed a titration model considering the heme perturbations caused by protonation of the amino acid side chains of the β-subunits contributing to the observed alkaline Bohr effect. The pK values of these groups were obtained from the analysis of the oxygen binding curves. The application of this protocol reveals that the protonation of two titrable groups (pK = 6.6 and 8.1 in the high affinity *r*-state) causes significant changes of the heme perturbation. The molecular basis of this effect is discussed in detail.

Theoretical background

1. Raman theory

A detailed description of the Raman theory employed in this study has been given elsewhere (Schweitzer-

Stenner and Dreybrodt 1985). In this paper we present only the basic equations for the vibronic coupling matrix elements used as free parameters in a fitting procedure.

Our theory is an extension of the PNSF-theory (Peticolas et al. 1970) which is based on Loudon's formalism in fifth-order (Loudon 1973). It considers contributions of the vibronic sidebands of the B- and Q-absorption bands by rationalizing the creation and subsequent annihilation of phonons giving rise to these bands. Symmetry perturbations of the heme due to asymmetric side chains and heme apo-protein contacts are introduced into this formalism by expanding the vibronic coupling operator in the Hamiltonian with respect to static normal distortions $\delta Q^{\Gamma'}$, classified due to the symmetry races of the Raman active vibrations in the D_{4h}-symmetry (i.e. A_{1g}, B_{1g}, B_{2g}, and A_{2g}). This leads to the following expression for the vibronic coupling matrix element:

$$c_{es}^{\Gamma} = \langle e|\, \mathrm{d}H/\mathrm{d}Q_R^{\Gamma} + \sum_{\Gamma'} \mathrm{d}^2H/\mathrm{d}Q_R^{\Gamma}\, \mathrm{d}Q^{\Gamma'}|s\rangle\, Q_{01}^{R}\, \delta Q^{\Gamma'} \quad (1)$$

where $|e\rangle$, $|s\rangle$ denote the excited electronic states related to the Q- and B-absorption bands. The operators $\mathrm{d}H/\mathrm{d}Q_R^{\Gamma}$ and $\mathrm{d}H^2/(\mathrm{d}H_R^{\Gamma}\, \mathrm{d}H^{\Gamma'})$ denote the vibronic coupling of the Raman mode in ideal D_{4h}-symmetry and its changes resulting from the perturbations of the heme moiety resulting from static normal distortions $\delta Q^{\Gamma'}$ respectively. Q_{01}^{R} is the transition matrix element of the Raman vibration.

Using this approach, analytic expressions for DPR and EPs result which contain the distortion parameters c_{es}^{Γ}. These are, to a first approximation, linearly related to the distinct normal distortions $\delta Q^{\Gamma'}$. They are used as free parameters in a fit of the analytical expressions to the experimental DPR-dispersion and EP curves.

2. *Allosteric model designed to analyse oxygen binding curves*

In order to analyse the oxygen binding curves of hemoglobin-NES we have applied an extension of the MWC-model (Monod et al. 1965) suggested by Herzfeld and Stanley (1974). The mathematical formalism of this theory and its application to hemoglobin trout IV have been reported in detail in an earlier work (Schweitzer-Stenner and Dreybrodt 1989). Therefore we confine ourselves to the introduction of the basic parameters and to the final equations of the employed theory.

First, we rationalize the energy contributions in the absence of ligands and effectors in the following way:

1. The tetrameric hemoglobin molecule can exist in two different states, T and R. In the T state the spatial arrangement of the four subunits is determined by a large number of non-covalent bonds among the subunits (Perutz 1970). A $T \rightarrow R$ transition is caused by rupture or weakening of these bonds and provides a more relaxed quaternary state. The energies of the T and R states are written as:

$$G_q = qG_q^0 \quad (2)$$

where $q = 1,2$ labels the T and R state respectively. G_q^0 denotes the energy difference between the two states.

2. The subunits containing the active sites for ligand and effector binding can exist in two different tertiary conformations r and t with different ligand binding affinities. Their energies are given by:

$$g_{\tau_j} = \tau_j g_{\tau_j}^0 \quad (3)$$

where $\tau_j = 1,2$ label the t and r states of the j^{th} subunit respectively, $g_{\tau_j}^0$ denotes the energy difference between the two tertiary states.

3. The MWC model is based on the assumption that all subunits exist in the same tertiary conformation, either in the r state when the tetramer is in the R configuration or in the t state, when the quaternary state is T. In order to consider mixed configurations – f.i. a quaternary T state where some of the subunits are still in the tertiary r state one has to introduce a quaternary-tertiary interaction energy given by:

$$G_{q\tau_j} = -(-1)^{(\tau_j + q)}\, G_{q\tau_j}^0 \quad (4)$$

where $G_{q\tau_j}^0$ denotes the energy difference between conformations r and t of subunit j in a given quaternary state q. As can be seen from Eq. (4), the $q\,\tau$ interaction energy is positive if $\tau_j = q$. If, however, the tertiary state is linked to the corresponding quaternary state ($\tau_j = q$), $G_{q\tau_j}$ becomes negative.

4. The MWC model completely neglects the fact that conformational changes in one subunit may induce variations in the adjacent ones (nearest neighbour interaction, Koshland et al. 1966). If one takes this into account, the following energy has to be introduced:

$$g_{\tau_j, \tau_{j+1}} = (-1)^{(\tau_j + \tau_{j+1})}\, g_{\tau_j, \tau_{j+1}}^0 \quad (5)$$

$g_{\tau_j, \tau_{j+1}}^0$ denotes the energy differences between different conformations, f.i. $t_j t_{j+1}$ and $t_j r_{j+1}$. Equation (5) shows that the nearest neighbour interaction energy is negative when the adjacent subunits are in the same tertiary conformation. Different tertiary conformations of neighbouring subunits, however, lead to positive energy values.

The total energy of the unliganded molecule can now be formulated using Eqs. (2)–(5). One obtains:

$$G_c = \sum_q \{q\, G_q^0 + \sum_j (\tau_j g_{\tau_j}^0 - (-1)^{\tau_j + q}\, G_{q\tau}^0) - \sum_j (-1)^{\tau_j + \tau_{j+1}}\, g_{\tau_j, \tau_{j+1}}^0\}. \quad (6)$$

Now we deal with the energy contributions resulting from ligand binding. The equilibrium constant of ligand binding to the prosthetic group of subunit j can be described by the following equations:

$$K_{t_j}^L = \exp\{-[-\mu_L + G_j^0 - G_{Lj}]\}/p_L \quad (7\,a)$$

$$K_{r_j}^L = \exp\{-[-\mu_L + G_j^0 + G_{Lj}]\}/p_L \quad (7\,b)$$

where $K_{t_j}^L$, $K_{r_j}^L$ denote the equilibrium constants due to the binding of the ligand L to the j^{th} subunit in the t and r state respectively. G_{Lj} represents half of the energy difference between the liganded r and t states and G_j^0 denotes the energy of ligand binding to the subunits, without considering their tertiary conformation. The chemical potential of the ligand is denoted by μ_L, p_L represents the partial pressure of the atmosphere of ligand L in contact with the solution.

Next we rationalize the binding of protons to those titrable groups, the protonation of which influences the equilibrium between both the quaternary T and R states (quaternary effector binding) and the tertiary t and r conformations (tertiary effector binding). The corresponding K-values are calculated by employing:

$$K_{l^T}^{H^+} = \exp[-(-\mu_H + G_{e,l}^{q,0} - G_{e,l}^q)/R\,T]/[H^+] \quad (8\,a)$$

$$K_{l^R}^{H^+} = \exp[-(-\mu_H + G_{e,l}^{q,0} + G_{e,l}^q)/R\,T]/[H^+] \quad (8\,b)$$

$$K_{m^{\tau T}}^{H^+} = \exp[-(-\mu_H + G_{e,m}^{q\tau,0} + G_{e,m}^{q\tau})/R\,T]/[H^+] \quad (8\,c)$$

$$K_{m^{\tau R}}^{H^+} = \exp[-(-\mu_H + G_{e,m}^{q\tau,0} - G_{e,m}^{q\tau})/R\,T]/[H^+] \quad (8\,d)$$

$$K_{jk^t}^{H^+} = \exp[-(-\mu_H + G_{e,j,k}^{\tau,0} - G_{e,j,k}^{\tau})/R\,T]/[H^+] \quad (8\,e)$$

$$K_{jk^r}^{H^+} = \exp[-(-\mu_H + G_{e,j,k}^{\tau,0} + G_{e,j,k}^{\tau})/R\,T]/[H^+] \quad (8\,f)$$

where $K_{l^T}^{H^+}$, $K_{l^R}^{H^+}$ denote the equilibrium constants of the l^{th} quaternary effector binding site in the T and R states, $K_{m^{\tau T}}^{H^+}$, $K_{m^{\tau R}}^{H^+}$ are the equilibrium constants of the m^{th} quaternay-tertiary effector binding sites and $K_{jk^t}^{H^+}$, $K_{jk^r}^{H^+}$ denote the equilibrium constants of the k^{th} tertiary effector binding site of the j^{th} subunit in the t and r states respectively.

The chemical potential of a proton in solution is μ_H, $[H^+]$ is the proton activity, $G_{e,l}^q$ represent half of the energy difference among the protonated R and T conformations, $G_{e,l}^{q\tau}$ denotes half of the energy difference between the protonated conformation of a tertiary structure which is matched to the quaternary state and the protonated conformation of the same but mismatched tertiary state conformation. $G_{e,j,k}^{\tau}$ denotes the energy difference between the protonated r and t states and $G_{e,l}^{q,0}$, $G_{e,j,k}^{\tau,0}$ are the corresponding effector binding energies, independent of the distinct conformations.

Finally we calculate the grand partition sum Z, the general definition of which is given by:

$$Z = \sum \exp\{[n\,\mu_L + n\,\mu_P - G_c - G_L - G_e]/R\,T\] \quad (9)$$

where n is the number of binding sites occupied in each state, μ_P is the chemical potential of the unoccupied protein and G_c is the conformational energy given by Eq. (6). The energy provided by ligand and effector binding which depends on the ligand and proton concentrations and is denoted by G_L and G_e respectively (c.f. Eqs (7) and (8)). The thermal energy is expressed in terms of the gas constant, R, and the absolute temperature, T.

The explicit formulation of the grand partition sum requires some length algebra which is presented in detail in another paper (Schweitzer-Stenner and Dreybrodt 1989). The final expression was used to calculate the saturation function of ligand binding by employing the equation:

$$Y = (4\,Z)^{-1}\,\mathrm{d}Z/\mathrm{d}(\mu_L/R\,T). \quad (10)$$

Both the equilibrium constants of ligand and effector binding and the energy differences between the different conformations of the unliganded molecule have been obtained by using them as free parameters in a fitting procedure to the experimental O_2-binding curves.

3. *Formulation of the effective polarizibility tensor*

From the DPR and EPs data parameters c_{es}^{Γ} (c.f. Eq. (1)) can be derived which result from incoherent superposition of Raman scattering of Hb-molecules in the distinct conformational states described above. Therefore the c_{es}^{Γ} have to be regarded as effective distortion parameters. Their values depend on the population of the different conformations. Thus as has been shown elsewhere (Schweitzer-Stenner et al. 1984 b), the Raman tensor can be regarded as an effective tensor the elements of which are expressed by:

$$\beta_{\mu\sigma,\,\text{eff}} = \{\sum_s X_s(\beta_{\mu\sigma})_s^2\}^{1/2} \quad (11)$$

where X_s denotes the mole fraction of the s^{th} conformation, the corresponding Raman tensor of which is provided by the tensor elements $(\beta_{\mu\sigma})_s$.

This leads to the following expression for the effective distortion parameters:

$$c_{es}^{\Gamma}(\text{pH}) = \{\sum_s X_s(c_{es}^{\Gamma})_s^2\}^{1/2} \quad (12)$$

$(c_{es}^{\Gamma})_s$ are the distortion parameters related to the distinct conformation s.

The mole fractions of the configurations of fully oxygenated Hb are given by the following equation:

$$X_s = \exp\{-\sum_j [G_s(\tau_j, q, \text{pH})/R\,T]\}/Z \quad (13)$$

$G_s(\tau_j, q, \text{pH})$ denotes the Gibbs' free energy of the conformation under consideration, s.

Inserting Eq. (13) into Eq. (12) we fitted the obtained pH-dependence of the distortion parameters by using the $(c_{es}^{\Gamma})_s$ as free parameters.

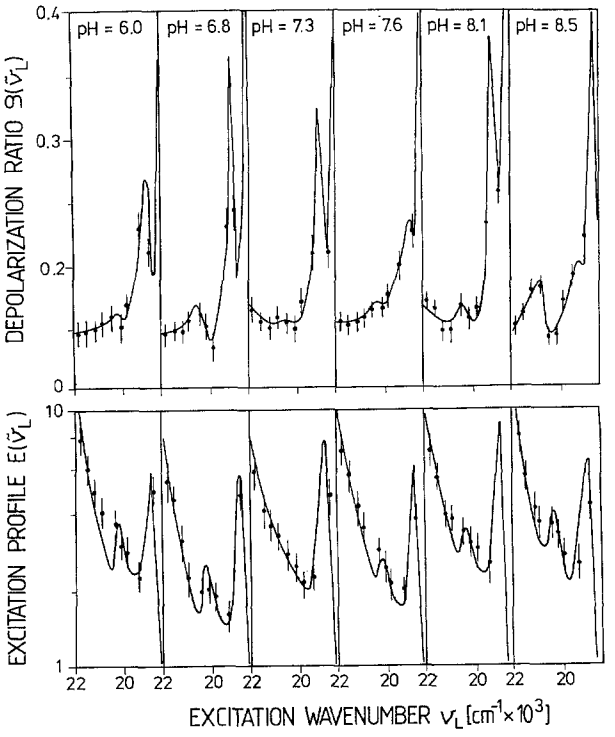

Fig. 1. DPR dispersion curves and EP of the 1,375 cm^{-1} (ν_4) mode of oxyHb-NES. The full lines result from the fitting procedure

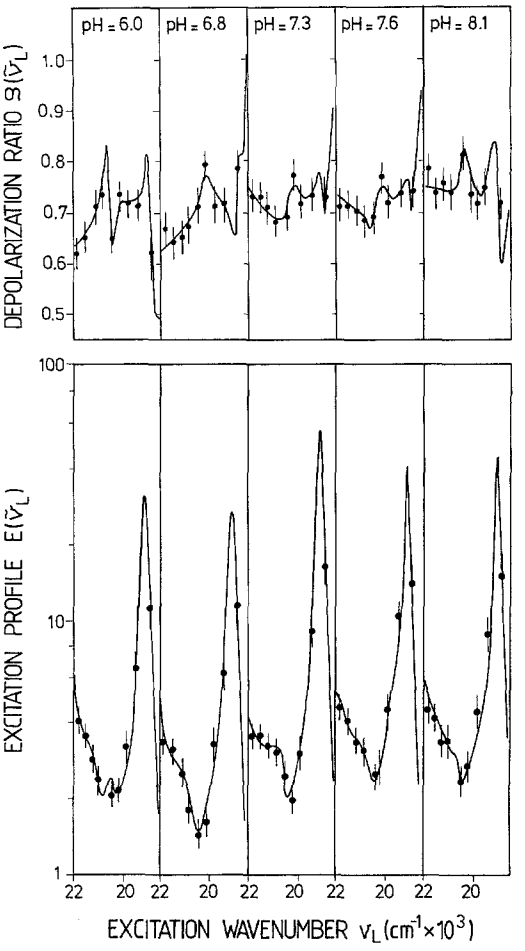

Fig. 2. DPR dispersion curves and EP of the 1,638 cm^{-1} (ν_{10}) mode of oxyHb-NES. The full lines results from the fitting procedure

For all computer fits we used a program called MINUITL from the CERN library. A detailed description of its mathematical basis and its application has been given elsewhere (James 1972; Schweitzer 1983).

Experimental

1. Material

Human adult hemoglobin was prepared from freshly drawn blood by standard procedures (Brunner et al. 1972). To obtain HbO_2-NES, N-ethyl-maleimide (NEM) was added to HbO_2 in a ratio 1 *M* NEM to 0.5 *M* HbO_2, and allowed to react for 24 h. To adjust the pH value the HbO_2-NES solution was dialyzed against 0.1 *M* bis-*tris* and *tris* buffers. The concentration was adjusted to 1 m*M* by measuring the optical absorbance with a Hewlett-Packard diode array spectrometer.

2. Method

The experimental set up designed to measure the polarized Raman spectra between 1,200 cm^{-1} and 1,700 cm^{-1} has been described in detail by el Naggar et al. (1985). The measured Raman spectra were digitized and stored on a microcomputer for further analysis. To calculate the correct height of the Raman lines a program was employed to subtract fluorescence background and to decompose complex spectra into distinct Lorentz lines of defined width and height. The relative intensities thus obtained were corrected for the frequency dependence, the transmission of the spectrometer and the power of the incident laser light. As has been demonstrated by el Naggar et al. (1985), corrections due to absorption and imaging errors are not necessary.

Results

1. DPR-dispersion and excitation profiles

Figure 1 shows the DPR-dispersion curves and the corresponding excitation profile ($E = E_\perp + E_\parallel$) of the 1,375 cm^{-1} oxidation marker line for different pH values between pH = 6.0 and 8.5.

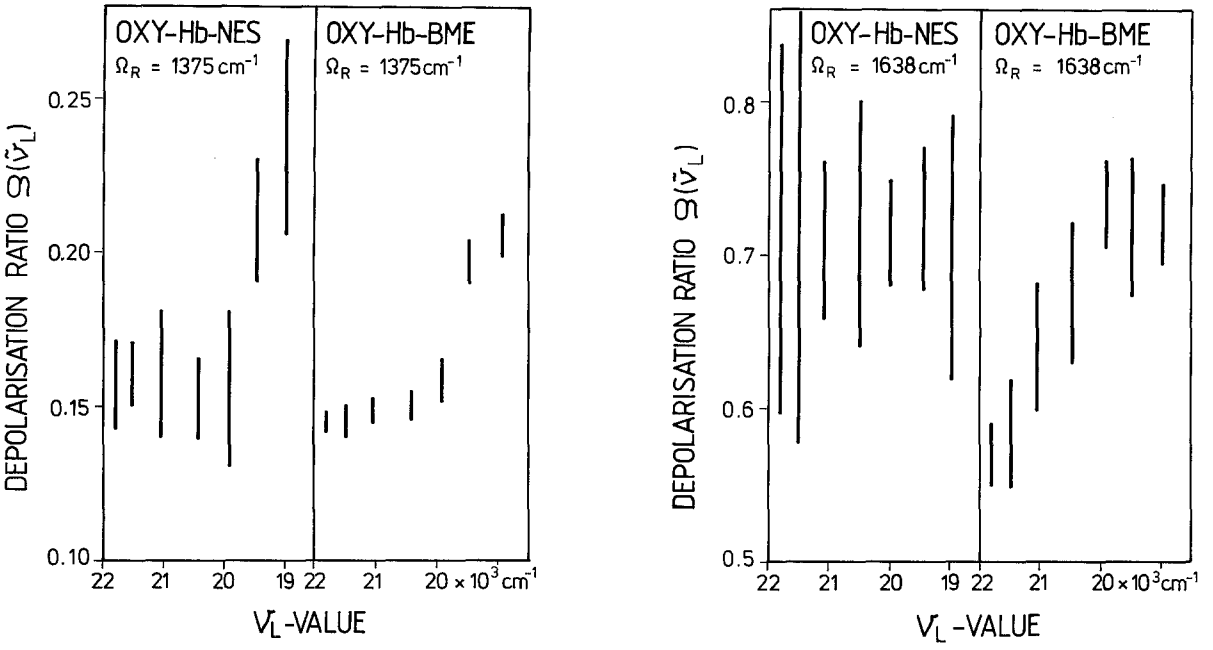

Fig. 3. Representation of the pH-induced DPR variations of both, the oxidation marker and the spin marker lines for oxyHb-NES and oxyHb-BME. The data for oxyHb-BME are taken from Wedekind et al. (1985)

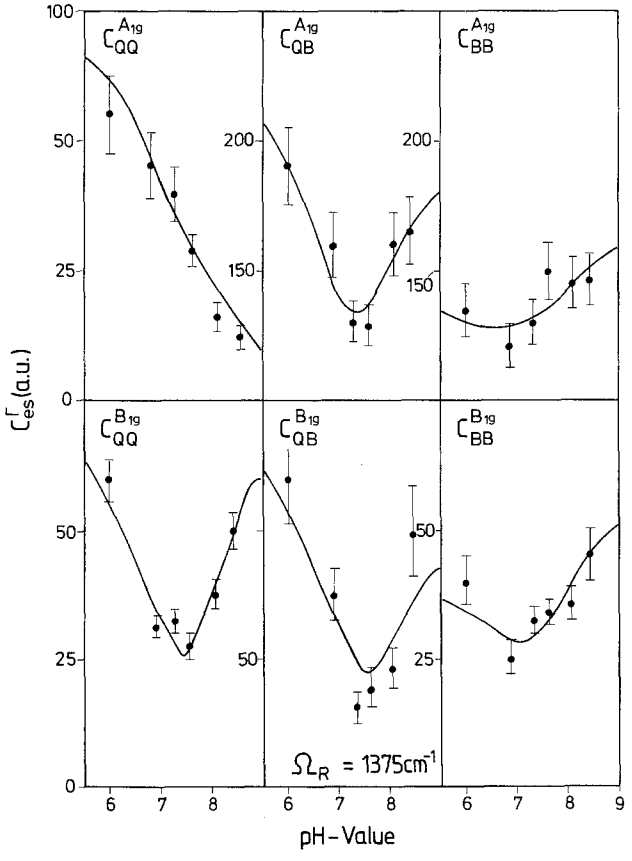

Fig. 4. $c^{I_{es}}$(pH) diagrams of the 1,375 cm^{-1} mode. The full lines result from the application of the titration model

The DPR show a pH-dependence, especially at 21,000 cm^{-1}, 19,000 cm^{-1} and 18,900 cm^{-1}. The spin-marker DPR (Fig. 2) does not exhibit such drastic changes between pH = 7.3 and 8.0. In the acid region (pH < 7.0) and the alkaline region (pH > 7.6), however, variations of the DPR dispersion have been obtained.

In order to demonstrate that these DPR variations are beyond the statistical error of the data, we have carried out a comparison with corresponding data observed for oxyHb-BME. As has been shown by Wedekind et al. (1985), the DPR dispersion curves of the oxidation and spinmarker mode of the oxyHb-BME Raman spectrum do not exhibit variations with pH larger than the experimental errors. Hence by comparing the variations of the DPR over the entire pH range of oxyHb-BME with those for oxyHb-NES for each excitation wavelength one can judge whether the observed variations in NES are larger than the experimental error. This is done in Fig. 3. The black bars mark the range of DPR observed in the investigated pH region for the indicated excitation wavelength. It is clear from this representation that the alterations of the DPR values observed for the oxyHb-NES Raman modes are significantly larger than the variations of the oxyHb-BME fundamentals.

To analyse the experimental data our theoretical formalism (Schweitzer-Stenner and Dreybrodt 1985) has been employed in a fitting procedure. The full lines

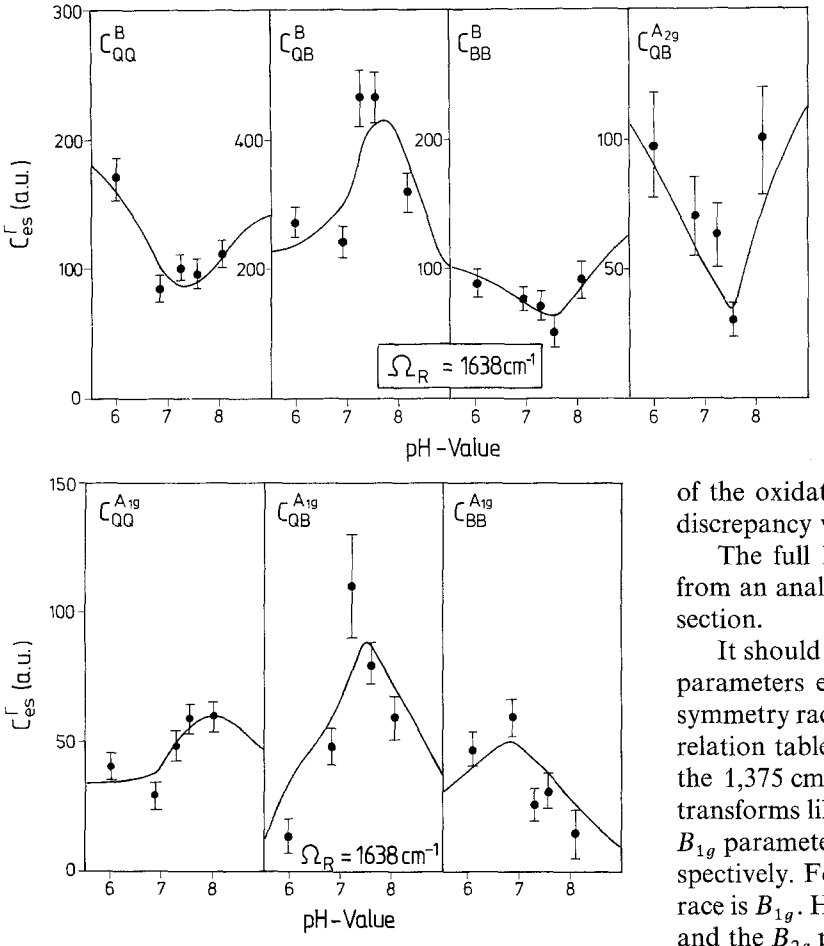

Fig. 5. $c^{\Gamma_{es}}$(pH) diagrams of the 1,638 cm^{-1} mode. The full lines result from the application of the titration model

in Figs. 1 and 2 display the curves resulting from this procedure.

The pH-dependence of the distortion parameters thus obtained are exhibited in Fig. 4 (1,375 cm^{-1}) and Fig. 5 (1,638 cm^{-1}). All parameters of the oxidation marker mode except c^{A1g}_{QQ} exhibit nearly the same shape: a minimum in the physiological region between 7.0 and 8.0 and an increase with increasing and decreasing pH values. This is similar to what has been obtained for oxyHbA at low Cl^- concentrations and for oxyHb-trout IV (Schweitzer-Stenner et al. 1986, 1989). The Franck Condon parameter c^{A1g}_{QQ}, however, shows a monotonic decrease with increasing pH. The reason for this behaviour will be discussed later in relation to Table 3. The corresponding parameters of the 1,638 cm^{-1} fundamental in Fig. 5 do not display such uniform behaviour: the parameters related to A_{1g} contributions are maximal at physiological pH and decrease upon approaching the alkaline and the acid region. The same behaviour has been established for the predominent parameter c^B_{QB}. The parameters c^B_{QQ} and c^B_{BB}, however, show a similar minimum to the c^{B1g}_{es} of the oxidation marker line. An explanation of this discrepancy will be given in the next section.

The full lines displayed in these diagrams result from an analysis which will be introduced in the next section.

It should be mentioned that the distinct distortion parameters exbibit the following relationship to the symmetry race of the respective distortion (c.f. the correlation table in Schweitzer-Stenner et al. 1984a): for the 1,375 cm^{-1} mode the undistorted normal mode transforms like A_{1g}. Therefore, the calculated A_{1g} and B_{1g} parameter are due to A_{1g} and B_{1g} distortions, respectively. For the 1,638 cm^{-1} line the normal mode race is B_{1g}. Hence the A_{1g} parameters result from B_{1g}, and the B_{2g} parameters from A_{2g} distortions. The B_{1g} parameters are related to both the undistorted Raman mode and A_{1g} distortions.

Since B_{1g} and B_{2g} contributions to the polarizibility tensor are difficult to differentiate, the respective distortion parameters have been added to c^B_{es}.

2. *Analysis of the oxygen binding curves*

The investigation of oxygen binding to both hemoglobin A and hemoglobin-NES was achieved by applying the allosteric model of Herzfeld and Stanley (1974) to oxygen binding curves measured by Shih et al. (1984) under the same experimental conditions.

The fits to the oxygen binding data were carried out according to the following protocol:

i) First, we performed a fit to the binding curves obtained for normal HbA. To reduce the number of free parameters we have taken the well known pK values of the two amino acid groups predominating in the alkaline Bohr effect (i.e. Val(NH1)α ($pK_{t\alpha}$, $pk_{r\alpha}$), His(HC2)β ($pK_{t\beta 1}$, $pK_{r\beta 1}$) from the literature (Kilmartin et al. 1980; Perutz et al. 1985) (c.f. Table 1). The acid Bohr effect can be neglected in our study. In accordance with the findings of Perutz et al. (1980) we have further assumed that another titrable group with

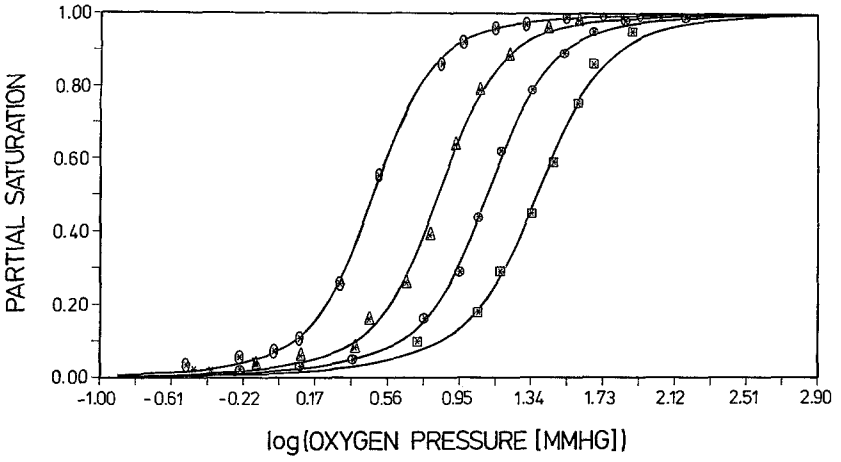

Fig. 6. O_2 binding curves of HbA measured at pH = 8.0, 7.4, 7.0 and 6.5. The full lines result from the fit to these data taken from Shih et al. (1984)

Table 1. Equilibrium constants and energy values of O_2 binding to hemoglobin A. The standard deviation taken from the on diagonal elements of the inverted Hesse matrix is denoted as error I. Error II results from error analysis carried out with the CONTOUR plots

A) Conformational energies

Energy type	Parameter values [kJ/mol]	Error I	Error II
G_q^0	3.8	± 3.0	± 3.0
$g_{\tau\alpha}^0$	10.4	± 0.6	± 1.0
$g_{\tau\beta}^0$	10.4	± 0.6	± 1.0
$G_{q\tau\alpha}^0$	1.9	± 0.6	± 0.7
$G_{q\tau\beta}^0$	2.9	± 0.6	± 0.7
$g_{\tau j, j+1}^0$	0	–	–

B) Equilibrium constants of O_2-binding

Constant	Parameter values $[\text{mmHg}]^{-1}$	Error I	Error II
$k_{t,\alpha}^L$	4.0×10^{-3}	$\pm 5.0 \times 10^{-3}$	$\pm 5.0 \times 10^{-3}$
$k_{t,\beta}^L$	4.0×10^{-3}	$\pm 5.0 \times 10^{-3}$	$\pm 5.0 \times 10^{-3}$
$k_{r,\alpha}^L$	65	± 8	± 20
$k_{r,\beta}^L$	65	± 8	± 20

C) pK-values of the effector binding sites

C1) tertiary effector pK in the unliganded state

pK-assignment	Parameter values	Error I	Error II
$pK_{t\alpha}$	8.2	–	–
$pK_{t\beta 1}$	7.8	–	–
$pK_{t\beta 2}$	7.1	± 0.6	± 0.6

C2) tertiary effector pK in the liganded state

pK-assignment	Parameter values	Error I	Error II
$pK_{r\alpha}$	7.1	± 0.7	± 0.7
$pK_{r\beta 1}$	6.6	–	–
$pK_{r\beta 2}$	6.5	± 0.5	± 0.5

$pK_{t\beta 2}$, $pK_{r\beta 2}$ contributes to the Bohr effect. Since its pK values in the r and t states are not well established, we used them as free parameters in the fitting procedure. All these Bohr groups were considered to be teritary effector binding sites. Furthermore we assumed that the equilibrium constants of oxygen binding and the tertiary energy differences are identical for the α and β subunits.

The fit to the O_2-binding curves thus obtained yields excellent agreement with the experimental data (c.f. Fig. 6). The calculated values of the free parameters are listed in Table 1. As one can see from this data set, the additional Bohr group exhibits a pK shift from $pK_{t\beta 2} = 7.1$ to $pK_{r\beta 2} = 6.5$. The quaternary-tertiary interaction energies $G_{q\tau,\alpha}^0$ and $G_{q\tau,\beta}^0$ are of the same order of magnitude as the thermal energy, in contrast to the MWC-model where it is assumed to be infinite. The $q\tau$ interaction energy related to the β subunits is a factor of 1.5 larger than that of the α subunits.

It is noteworthy in this context that a similar, but much more pronounced asymmetry between the $q\tau$ interactions related to the α and β subunits has been obtained for oxyHb-trout IV (Schweitzer-Stenner and Dreybrodt 1989). Thus one concludes that structural changes of the β subunits (i.e. $t \rightarrow r$ transitions, protonation processes) make a dominant contribution to the quaternary $T \rightarrow R$ transition. This is in accordance with the results obtained from a stereochemical investigation on the quaternary structure change of HbA in the ligation process, which has been reported recently by Arata et al. (1988).

It is noteworthy that no evidence has been found for the existence of interactions between adjacent subunits (i.e. the nearest neighbour – interaction energy is negligible).

The parameters obtained from the fit to the O_2-binding curves of HbA have been partially used to fit the O_2-binding curves of hemoglobin-NES in the following way: It is well known that the structural modifications caused by the binding of NEM to the

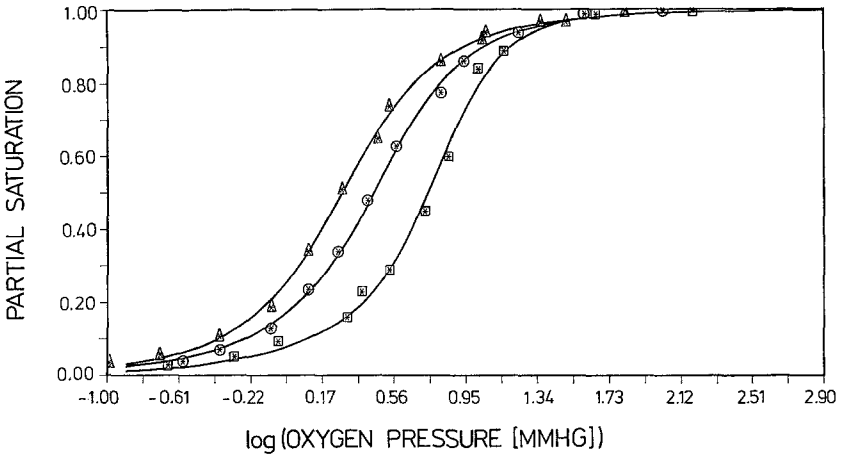

Fig. 7. O_2 binding curves of Hb-NES measured at pH = 9.0, 7.4, and 6.4. The full lines result from the fit to these data taken from Shih et al. (1984)

protein do exclusively affect the β subunits. Therefore we have used all parameters related to the α subunits from the fit to the binding curves of the unmodified HbA (i.e. $k_{t\alpha}^L$, $k_{r\alpha}^L$, $g_{\tau\alpha}$, $G_{q\tau,\alpha}^0$ and the pK values of Val(NH1)α ($pK_{t\alpha}$, $pK_{r\alpha}$ in Table 1) as fixed parameters. We also fixed the value of $K_{t,\beta}^L$. This is reasonable since a sensitivity analysis showed that variations of $K_{t,\beta}^L$ between 10^{-2}(mmHg)$^{-1}$ and 10^{-3}(mmHg)$^{-1}$ do not affect the oxygen binding curves within the limits of experimental accuracy.

Despite these restrictions an excellent reproduction of the experimental data is achieved. It is displayed by the full lines in Fig. 7. The corresponding values of the remaining fitting parameters are listed in Table 2.

In contrast to what has been established for HbA, the *r* state tertiary energies of the α and β subunits are not identical, since the modification with NEM has affected only the β subunits. Furthermore, NEM binding lowers the quaternary energy G_q^0 and the quaternary-tertiary interaction energy $G_{q\tau,\beta}^0$ thus causing a decrease of the degree of cooperativity. The most interesting result, however, concerns the interpretation of the reduced Bohr effect of the molecule: the fit reveals that instead of the contribution provided by the protonation of His(HC1)β ($pK_{t\beta1} = pK_{r\beta1}$) another amino acid group in the β subunit exhibits an inverse Bohr effect ($pK_{t\beta3} = 6.7$, $pK_{r\beta3} = 8.1$). Omitting this positive pK shift yields unsatisfactory fits. The pK values of the other Bohr group of the β subunit remain unchanged ($pK_{t\beta2} = 7.1$, $pK_{r\beta2} = 6.5$). The inverse Bohr effect provided by the third, oxyHb-NES specific Bohr group is partially compensated by the pK shift of a quaternary effector binding site ($pK_T = 6.9$, $pK_R = 5.6$) which causes a significant increase of both the effective quaternary energy G_q and the $q\tau$-interaction energy upon approaching the acid region. This finding is in accordance with the observed change of the cooperativity of O_2 binding to Hb-NES.

A detailed discussion of the binding properties of modified hemoglobins will be given in a future paper.

3. Error analysis of the fits to the oxygen binding curves

The program MINUITL contains three different minimizing subroutines named SEEK, SIMPLX and MIGRAD to search a local minimum of the chi-square function.

The standard deviation of the calculated parameter values were derived by MIGRAD as follows: The routing approximates the chi-square function near to its minimum by a paraboloid with comparable diameter in the different parameters centered at the minimum. The standard deviation is provided by the square root of the on-diagonal elements of the inverted Hesse-matrix derived at the minimum. The results of this calculation are listed as error I in Tables 1 and 2.

The model to be fitted however, is not linear. Hence the chi-square function may not be approximated very well by a paraboloid as described above. In this case the standard deviations calculated from the parabolic approximation do not represent the real statistical error. To obtain an upper limit for the real statistical error we employed the subroutine CONTOUR of the MINUITL program designed to calculate the projection of the chi-square function on a two dimensional subspace of the parameter space. From this representation one derives error values which may be different from those obtained from the Hesse matrix of the symmetric paraboloid. We have applied the CONTOUR-routine to all parameters which exhibit a high degree of correlation. The degree of correlation can be obtained from the off-diagonal elements of the inversed Hesse matrix. The errors thus calculated are listed as error II in Tables 1 and 2.

The application of this procedure yields comparatively large errors for pK_R, $pK_{t\beta2}$, $pK_{r\beta2}$ ($j = \alpha, \beta$) and G_q^0. The standard deviation (error I) of $K_{t,j}^L$ is significantly smaller than the corresponding error II. The corresponding CONTOUR-plots of these parameters reveal that this is due to significant correlation effects *a)* between all parameters related to the quaternary

Table 2. Equilibrium constants and energy values of O_2 binding to hemoglobin-NES. The standard deviation taken from the on diagonal elements of the inverted Hesse matrix is denoted as error I. Error II results from error analysis carried out with the CONTOUR plots

A) Conformational energies

Energy type	Parameter values [kJ/mol]	Error I	Error II
G_q^0	1.0	±0.7	±0.7
$g_{\tau\alpha}^0$	10.4	±0.6*	±1.0*
$g_{\tau\beta}^0$	13.1	±0.3	±0.4
$G_{q\tau\alpha}^0$	1.9	±0.6*	±0.7*
$G_{q\tau\beta}^0$	0.7	±0.2	±0.7
$g_{\tau j, j+1}^0$	0	–	–

B) Equilibrium constants of O_2-binding

Constant	Parameter values $[mmHg]^{-1}$	Error I	Error II
$k_{t,\alpha}^L$	4.0×10^{-3}	$\pm 5.0 \times 10^{-3}$*	$\pm 5.0 \times 10^{-3}$*
$k_{t,\beta}^L$	4.0×10^{-3}	$\pm 5.0 \times 10^{-3}$*	$\pm 5.0 \times 10^{-3}$*
$k_{r,\alpha}^L$	65	±8*	±20*
$k_{r,\beta}^L$	70.6	±9	±20

C) pK-values of the effector binding sites

C1) tertiary effector pK in the unliganded state

pK-assignment	Parameter values	Error I	Error II
$pK_{t\alpha}$	8.2*	–	–
$pK_{t\beta 2}$	7.1	±0.6	±0.6
$pK_{t\beta 3}$	6.6	±0.3	±0.3

C2) tertiary effector pK in the liganded state

pK-assignment	Parameter values	Error I	Error II
$pK_{r\alpha}$	7.1*	–	–
$pK_{r\beta 2}$	6.6	±0.6	±0.6
$pK_{r\beta 3}$	8.1	±0.1	±0.2

D) pK-values of a quaternary effector binding site

pK-assignment	Parameter values	Error I	Error II
pK_T, $pK_{T\tau}$	6.9	±0.4	±0.5
pK_R, $pK_{R\tau}$	5.6	±0.7	±0.9

* These values were obtained from the fit to the oxygen binding curves of HbA

transition process and *b)* between $K_{r,j}^L$ and the tertiary energy $g_{\tau j}^0$ related to the ligand affinity of the j^{th} subunit.

It is finally noteworthy that the errors obtained for $pK_{t\beta 3}$ and $pK_{r\beta 3}$ (cf. Table 2) are comparatively small.

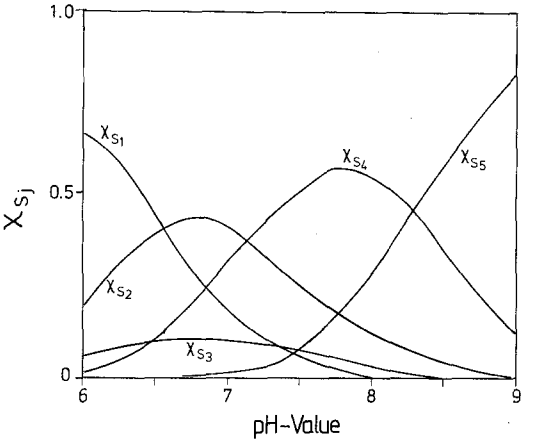

Fig. 8. Mole fractions of the predominant conformations of oxyHb-NES in dependence on the pH value

This corroborates the observation of an inverse Bohr effect influencing O_2 binding to Hb-NES.

4. pH-dependence of the distortion parameters

Now the tools are available to investigate the pH-dependence of the distortion parameters displayed in Fig. 4 (1,375 cm^{-1}) and Fig. 5 (1,638 cm^{-1}). First we employ Eq. (13) to calculate the mole fractions of all conformations of the fully oxygenated Hb-NES molecule. Figure 8 shows the pH-dependent mole fractions of the predominant conformations for illustration. Only five conformations have to be taken into account, since all the others show only negligibly small mole fractions. The dominant species are:

$$S_1 = \{R, r_\alpha, r_\alpha, r_\beta, r_\beta\}\ [1, 1, 1]$$
$$S_2 = \{R, r_\alpha, r_\alpha, r_\beta, r_\beta\}\ [1, 0, 1]$$
$$S_3 = \{R, r_\alpha, r_\alpha, r_\beta, r_\beta\}\ [1, 0, 0]$$
$$S_4 = \{R, r_\alpha, r_\alpha, r_\beta, r_\beta\}\ [0, 0, 1]$$
$$S_5 = \{R, r_\alpha, r_\alpha, r_\beta, r_\beta\}\ [0, 0, 0]$$

where $\{q, \tau_1, \tau_2, \tau_3, \tau_4\}\ [i_{\alpha 1}, j_{\beta 2}, j_{\beta 3}]$ is related to the quaternary state q, the tertiary states τ_j of the j^{th} subunit and the proton occupation numbers $i_{\alpha 1}$, $j_{\beta 2}$, $j_{\beta 3} = 0, 1$) of the three titrable tertiary effector groups. Evidence is provided that the pH-induced variation of the DPR dispersion of the considered oxyHbA-Raman lines is exclusively due to protonation processes occuring in the β subunits (Schweitzer-Stenner et al. 1986; Wedekind et al. 1985). Therefore we have neglected the influence of the protonation state of Val(NH1)α ($pK_{r\alpha} = 7.1$). Hence only three distinct conformations of the heme moiety exist: one due to the species S_1, a second due to S_2 and S_4 and a third due to S_3 and S_5 titration states, these are summarized as:

$T_1 = S_1 = [1, 1]$

$T_2 = S_2 + S_4 = [0, 1]$

$T_3 = S_3 + S_5 = [0, 0]$

where $[i_{\beta 2}, j_{\beta 3}]$ is related to the occupation numbers of the amino acid groups with pK = 6.6 and 8.2 respectively, which are either protonated or unprotonated in the β chains.

Second we relate each such titration state of the hemoglobin molecule to a distinct set of distortion parameters $c^{\Gamma}_{es}[i_{\beta 1}, j_{\beta 2}]$. Thus the effective parameters c^{Γ}_{es}(pH) obtained from our Raman experiments can be written as:

$$c^{\Gamma}_{es}(\mathrm{pH}) = \{X_1 (c^{\Gamma}_{es}[1, 1])^2 + X_2 (c^{\Gamma}_{es}[0, 1])^2 + X_3 (c^{\Gamma}_{es}[0, 0])^2\}^{1/2} \quad (14)$$

where X_1, X_2, and X_3 relate to the configurations T, T_2, and T_3 respectively. The parameters $c^{\Gamma}_{es}[i_{\beta 1}, j_{\beta 2}]$ are used as free parameters in order to fit the obtained c^{Γ}_{es}(pH) diagrams, whereas all pK values and the other thermodynamic constants considered in the titration model are provided by the fits to the O_2 binding curves for HbA and Hb-NES.

The results of the fits are displayed by full lines in Figs. 4 and 5. Sufficient agreement, especially with the data related to the 1,375 cm^{-1} data set, is established. Thus, evidence is provided that the protonation of the Bohr groups obtained from the fit to the binding curves of Hb-NES (pK = 6.6; 8.2) are responsible for the variations of the heme distortions reflected by the Raman data investigated.

The measured distortion parameters of the distinct conformations T_s are listed in Table 3. They are related to the c^{Γ}_{es}(pH) diagrams in Figs. 4 and 5 as follows: If $c^{\Gamma}_{es}[1, 0]$ is lower than $c^{\Gamma}_{es}[0, 0]$ and $c^{\Gamma}_{es}[1, 1]$ the effective parameter value is minimal at pH = 7.5 (Fig. 4, c^{A1g}_{QB}-c^{B1g}_{BB}). Correspondingly one obtains a maximal c^{Γ}_{es}(pH) value if $c^{\Gamma}_{es}[1, 0] > c^{\Gamma}_{es}[0, 0]$, $c^{\Gamma}_{es}[1, 1]$ (c^{A1g}_{QB} and c^{B}_{QB} in Fig. 5a and b respectively). Finally a monotonic increase of c^{Γ}_{es}(pH) towards the acid region is due to $c^{\Gamma}_{es}[1, 1] < c^{\Gamma}_{es}[1, 0] < c^{\Gamma}_{es}[0, 0]$ (c^{A1g}_{QQ} in Fig. 4).

Table 3. Distortion parameters $c^{\Gamma_{es}}[i_{\beta 2}, j_{\beta 3}]$ of the titration states resulting from the fit to the $c^{\Gamma_{es}}$ (pH) diagrams of the 1,375 cm^{-1} and the 1,638 cm^{-1} Raman fundamentals

A) 1,375 cm^{-1}

Conformations	c^{A1g}_{QQ}	c^{A1g}_{QB}	c^{A1g}_{BB}
$T_1 = [1, 1]$	70	210	131
$T_2 = [0, 1]$	27	103	125
$T_3 = [0, 0]$	5	190	162
Conformations	c^{B1g}_{QQ}	c^{B1g}_{QB}	c^{B1g}_{BB}
$T_1 = [1, 1]$	70	122	55
$T_2 = [0, 1]$	10	10	20
$T_3 = [0, 0]$	65	81	38

A) 1,638 cm^{-1}

Conformations	c^{A1g}_{QQ}	c^{A1g}_{QB}	c^{A1g}_{BB}
$T_1 = [1, 1]$	42	10	20
$T_2 = [0, 1]$	20	220	70
$T_3 = [0, 0]$	41	20	5
Conformations	c^{Bg}_{QQ}	c^{Bg}_{QB}	c^{Bg}_{BB}
$T_1 = [1, 1]$	179	232	101
$T_2 = [0, 1]$	22	603	69
$T_3 = [0, 0]$	148	150	133

Discussion

1. The pH-dependence of heme-apoprotein interactions

As we have shown in earlier papers (Wedekind et al. 1985, 1986; Schweitzer-Stenner et al. 1986, 1989), the two Raman fundamentals investigated are affected by different types of heme apoprotein interactions. These can be classified as follows:

The oxidation marker mode (1,375 cm^{-1}) is predominantly influenced by interactions between the proximal imidazole and the pyrrole nitrogens because of the large vibrational amplitudes of the N-C_α stretching vibration (Abe et al. 1978). This type of interaction causes an asymmetric perturbation of the heme core, when the imidazole is bent into a tilt position with respect to the heme plane (c.f. Warshel 1977; Gellin and Karplus, 1979). Therefore we relate a pH-dependent increase of the distortion parameters of the 1,375 cm^{-1} fundamental (ν_4-mode in the notation of Abe et al. (1978)) with the pH value to a conformational change of the proximal histidine from a symmetric to a tilt position relative to the plane of the porphyrin molecule. This structural variation effects an increase of the ligand dissociation constant (Friedman et al. 1984, Schweitzer-Stenner et al. 1986, 1989).

This model can be used as a rationale for the c^{Γ}_{es}(pH) diagrams of the ν_4 mode. As one can see from Table 3, the two established protonation processes influence the heme structure in an opposite way: The protonation of the amino acid group with $pK_{r\beta 2} = 8.1$ reduces both the A_{1g} and the B_{1g} type perturbations. Therefore at physiological pH values the imidazole is in a more symmetric position with respect to the heme chromophore compared with that in the alkaline region. The protonation in the acid region ($pK_{r\beta 1} = 6.6$), however, causes a strong increase of both types of heme distortions, which is due to a more tilt position of the proximal imidazole. Thus our results predict an increase of O_2 dissociation upon approaching both the acid and the alkaline region.

In contrast to the oxidation marker mode the symmetry properties of the *spin marker fundamental at*

1,638 cm^{-1} are mainly affected by coupling processes between the heme side chains and amino acid residues of the heme moiety (Wedekind et al. 1985), because its normal vibration (ν_{10} mode in the notation of Abe et al. 1978) can be described as a superposition of C_α, C_m stretching modes and large vibrations of the peripheral C_β atoms, nearly parallel to the C-C bonds between the C_β atoms and the porphyring side chains. Wedekind et al. (1985, 1986) provided experimental evidence that the protein side chain interaction affecting the vibronic properties of the ν_{10} mode does not influence the ν_4 mode significantly. Minor influences of the imidazole-heme interaction on the $_{10}$ fundamental, however, can be expected.

Stereochemical investigations have established evidence that the most relevant of the peripheral heme-apoprotein interactions is provided by the van der Waals contact between Val(FG5)β and the vinyl group of pyrrole 3 (Gellin and Karplus 1977). It is reasonable to assume that conformational changes of this interface are reflected by the symmetry distortion parameters of the porphyrin Raman fundamentals becuase π-electrons of the vinyl groups interacts with the π-electron system of the porphyrin (Hsu 1970).

The extent of the distortion depends on the orientation of the vinyl groups with respect to the heme plane, which is adjusted by the van der Waals contacts with the amino acid groups of the heme cavity. If the angle between the vinyl group and the heme is minimal, one obtains a maximal perturbation of the electronic properties of the heme. This perturbation is reduced if the vinyl is in a more out of plane configuration.

As one can see from Fig. 5 and Table 3, the two observed protonation processes influence the distinct distortions of the ν_{10} mode in a different manner:

The A_{1g} type distortion parameters, which are due to asymmetric B_{1g} distortions, exhibit a maximum in the physiological region and decrease significantly towards acid and alkaline pH. This reflects an increase of B_{1g} perturbations upon the protonation of the amino acid group with pK = 8.1 and a reduction of this perturbation type upon protonation of the amino acid group with pK = 6.6.

Since A_{1g} and A_{2g} perturbations contribute to the c_{es}^B parameters of the ν_{10} mode, the corresponding c_{es}^I(pH) values do not display the same qualitative dependence on the pH value as the parameters c_{es}^{A1g}(pH), which are exclusively due to B_{1g} distortions. The parameters c_{QQ}^B and c_{BB}^B are minimal in the physiological region and increase slighty towards the acid and alkaline region, in the same way as the c_{es}^I(pH) diagrams of the ν_4 mode. The predominant c_{QB}^B parameter, however, shows the same behaviour as the A_{1g} type contributions. It is therefore reasonable to relate the parameters c_{QQ}^B and B_{BB}^B to A_{1g} type distortions caused by the interaction between the proximal imidazole and the heme, whereas the large c_{QB}^B parameter reflects antisymmetric A_{2g} perturbations induced by the side chain-protein interactions.

Using the vinyl-Val(FG5) interaction as a key for the interpretation of the B_{1g} and A_{2g} perturbations affecting the ν_{10} fundamental, the following stereochemical picture can be obtained from our data: The protonation of the amino acid group with $pK_{r\beta 2} = 8.1$ pushes Val(FG4)β towards the vinyl group of pyrrole 3, which causes a decrease in the angle between the vinyl group and the heme plane and thus an increase of asymmetric heme perturbations. The protonation of the amino acid group with $pK_{r\beta 1} = 6.6$ counteracts this process: it forces the vinyl into an out of plane position thus decreasing the asymmetric heme perturbations.

2. *Assignment of the pK-values*

As we have shown above, three amino acid groups serve as tertiary effectors in hemoglobin NES. In the α subunits Val(NH1)α exhibits a pK shift from 8.1 to 7.1 upon $t \rightarrow r$ transition. In the β subunits His(HC3)β does not act as a teritary effector anymore, as is shown by the results listed in Table 2. This is in accordance with findings of Moffat (1971) and Kilmartin et al. (1980) reporting that the saltbridge between His(HC1)β and Asp(FG1)β is ruptured even in the t state by the binding of NEM to Cys(F9)β. The other Bohr group of the HbAβ subunits, which shifts its pK value from $pK_{t\beta 2} = 7.1$ to $pK_{r\beta 2} = 6.6$ is not influenced by the NEM-modification. This Bohr group has been attributed to Lys(EF6)β by Perutz et al. (1980). Since this group is located in the hinge region between the E and the F helix of the β subunits its protonation may affect the position of the F helix with respect to the C-terminal end. This would influence the equilibrium between the deoxy and the oxy-like conformation of the phenyl ring of Tyr(HC2)β thus affecting the FG and F helix via the H-bond between Tyr(HC2)β and Val(FG5)β and the steric coupling between the Tyr(HC2)β and the SH group of Cys(F9)β respectively (Shaanan 1983). The conformational changes of Val(FG5)β can be expected to induce heme perturbations via the interactions with the vinyl group of pyrrole 3 (detected by the ν_{10} mode). A structural variation of Cys(F9)β will most probably affect the interaction between the heme core and the imidazole of the adjacent histidine. DeYoung et al. (1976) have shown, that the Bohr-effect of the r state is absent in des(HisHC2)β-des(Tyr(HC1)β-HbA. Thus a direct influence on the conformation of the chromophore can be exluded for the oxygenated molecule.

Due to our analysis of the c_{es}^{Γ}(pH) diagrams the protonation of the amino acid group with $pK_{r\beta 2} = 6.6$ increases the asymmetric perturbations of the heme core by pushing the proximal histidine into a tilt position and furthermore it reduces the asymmetric perturbation of the peripheral part of the heme by increasing the angle between the vinyl group of pyrrole 3 and the heme plane. Assuming the above assignment of $pK_{r\beta 2}$ to Lys(EF5)β, a transfer mechanism with the following steps emerges from our data: Proton binding to Lys(EF5)$\beta \rightarrow$ variation of the orientation of the F/FG helix with respect to the C-terminal end $\rightarrow$ conformational change of the phenyl ring of Tyr(HC1)$\beta \rightarrow$ *a)* conformational change of Val(FG5)β which effects an alteration of the vinyl orientation relative to the heme plane and *b)* conformational change of the SH group of Cys(F9)β which leads to a more tilt position of the proximal imidazole.

The assignment of the amino acid group of the β subunits exhibiting an inverse Bohr effect in Hb-NES is more difficult. In contrast to what has been obtained for the other Bohr groups, this amino acid exbibits a large, positive pK shift from $pK_{t\beta 3} = 6.6$ to $pK_{r\beta 3} = 8.1$ thus counteracting the contributions of the other Bohr groups. The most reasonable explanation for this finding can be given by assuming that an imidazole of a histidine donates an H-bond to an acceptor group located in its environment. The existence of such an H-bond between His(FG5)β and Cys(F9)β has already been postulated by Moffat et al. (1971) who reinvestigated the X-ray data of oxyHb-NES by Perutz (1969). This prediction, however, has been questioned, because of the low resolution of the X-ray study (5 Å) (Shaanan, personal communication).

The pH-dependence of the distortion parameters obtained from the investigation of both the ν_4 and the ν_{10} mode, however, supports the interpretation of Moffat et al. (1971) for the following reasons:

a) The application of our titration model reveals that the protonation with $pK_{r\beta 3} = 8.1$ causes a significant variation of the heme perturbations. A similar effect has not been obtained for oxyHbA (Schweitzer-Stenner et al. 1986). This difference between oxyHbA and oxyHbA-NES gives evidence that the corresponding amino acid is located close to the NEM binding site (i.e. Cys(F9)β).

b) Therefore we conclude, that the $pK_{r\beta 3}$ values due to an immidazole group, because an alternative residue with comparable pK does not exist in the region of the F- and FG-helix.

c) The significant changes of all distortion parameters in the alkaline region support the existence of a H-bond which will be ruptured upon deprotonation of the corresponding imidazole. The quaternary effector in Hb-NES resulting from the fit to O_2 binding curves shows a shift of its pK value from $pk_T = 6.9$ to $pK_R = 5.6$. It cannot be excluded that this large pK shift is due to smaller contributions from several amino acid groups influencing the quaternary equilibrium. Further investigations are necessary to clarify this point.

We summarize our results as follows:

1. We have examined the DPR-dispersion of the oxidation marker (1,375 cm^{-1}) and the spin marker (1,638 cm^{-1}) lines of the oxyHb-NES Raman spectrum, which has been measured at different pH values between 6.0 and 8.5. From this we obtained the pH-dependence of symmetry classified A_{1g} and B_{1g} perturbations for the 1,375 cm^{-1} mode and A_{1g}, B_{1g} and A_{2g} distortions for the 1,638 cm^{-1} fundamental.

2. The pH-dependence of heme distortions thus obtained was rationalized in terms of a titration model which relates each conformation of the molecule to a distinct set of distortion parameters. The thermodynamic constants determining the equilibrium between the molecular conformations (i.e. the pK values of tertiary effector groups) were obtained from a fit to O_2 binding curves of Hb-NES carried out using an allosteric model of Herzfeld and Stanley (1974).

3. The following correlations between titration processes in oxygenated β subunits and structural variations of the heme chromophore could be proposed:

– protonation of a Bohr group with $pK_{r\beta 1} = 6.6$ (probably Lys(EF5)β) induces asymmetric perturbations into the heme core by switching the proximal imidazole into a tilt position with respect to the heme plane. Simultaneously it reduces the asymmetric distortion reflected by the 1,638 cm^{-1} mode by an increase of the angle between the vinyl group of pyrrole 3 and the heme plane

– the opposite effect occurs on protonation of another Bohr group with $pK_{r\beta 2} = 8.1$: the perturbation of the heme core is reduced (symmetric position of the proximal imidazole) whereas the distortions caused by heme side-chain-protein contacts is increased (predominantly the contact between the vinyl of pyrrole 3 and Val(FG4)β).

Acknowledgement. We would like to thank Dr. Boaz Shaanan (Weizmann Institute, Rehovot, Israel) for providing constructive criticsm on an earlier version of this paper. Furthermore we gratefully acknowledge the technical assistance of Mr. G. Ankele.

References

Arata Y, Seno Y, Jinay O (1988) A study on the quaternary structure change of hemoglobin in the ligation process. Biochim Biophys Acta 956:243–255

Abe M, Kitagawa T, Kyogoku Y (1978) Resonance Raman spectra in octaethylporphyrin-Ni(II) and mesodeuterated and ^{15}N-substituted derivatives. II. A normal coordinate analysis. J Chem Phys 69:4526–4534

Brunner H, Mayer A, Sussner H (1972) Resonance Raman scattering on the Haem Group of Oxy- and Deoxyhaemoglobin. J Mol Biol 70:153–156

Brunzel U, Dreybrodt W, Schweitzer-Stenner R (1986) pH-dependent absorption in the *B*- and *Q* bands of oxyhemoglobin and chemically modified oxyhemoglobin (BME) at low Cl^--concentration. Biophys J 49:1069–1076

De Young A, Pennely R, Tan-Wilson A, Noble RW (1976) Kinetic studies on the binding affinity of human hemoglobin for the 4th carbon monoxide molecule L_4. J Biol Chem 251:6692–6698

Friedman JM, Scott TW, Stepanowski RA, Ikedo-Saito M, Cone RL (1983) The iron-proximal histidine linkage and protein control of oxygen binding in hemoglobin. J Biol Chem 258:10564–10572

Gellin BT, Karplus M (1977) Mechanism of tertiary structural change in hemoglobin. Proc Natl Acad Sci USA 74:801–805

Herzfeld J, Stanley E (1974) A general approach to cooperativity and its application to the oxygen equilibrium of human hemoglobin and its effectors. J Mol Biol 82:231–265

Hsu MC (1970) Optical activity of heme proteins. PhD-thesis, Urbana, Illinois

Kilmartin JV, Fogg JH, Perutz MF (1980) Role of C-terminal histidine in the alkaline Bohr effect of human hemoglobin. Biochemistry 19:3189–3193

Koshland DE, Nemethy G, Filer D (1966) Comparison of experimental binding data and theoretical models in proteins containing subunits. Biochemistry 5:365–385

Kwiatkowski L, Noble RW (1982) The contribution of histidine (HC3)(146)β to the *R*-state Bohr effect in human hemoglobin. J Biol Chem 257:8891–8895

Loudon R (1973) The quantum theory of light. Clarendon Press, Oxford

Moffat JK (1971) Structure and functional properties of chemically modified horse hemoglobin. J Mol Biol 58:79–88

Monod J, Wyman J, Changeux JPC (1965) On the nature of allosteric transitions: a plausible model. J Mol Biol 12: 88–118

el Naggar S, Dreybrodt W, Schweitzer-Stenner R (1985) Haem-apoprotein interactions detected by resonance Raman scattering in Mb- and Hb-derivatives lacking the saltbridge His 146 β–Asp 94 β. Eur Biophys J 12:43–49

Perutz MF (1969) The haemoglobin molecule. Proc R Soc B 173:113–140

Perutz MF (1970) Stereochemistry of cooperative effects in haemoglobin. Nature (London) 228:726–734

Perutz MF, Kilmartin JV, Nishikura K, Fogg JH, Butler PJG (1980) identification of residues contributing to the Bohr effect of human hemoglobin. J Mol Biol 138:649–670

Perutz MF, Gronenborn AM, Clore GM, Fogg JH, Shih Tb (1985) The pK_a-values of two histidine residues in human hemoglobin, the Bohr effect and the dipole moment of the α-helix. J Mol Biol 183:491–498

Peticolas W, Nafie I, Stein P, Fanconi B (1970) Quantum theory of the intensities of molecular vibrational spectra. J Chem Phys 52:1576–1588

Schweitzer R (1983) Untersuchung von pH-induzierten Symmetrieverzerrungen der prosthetischen Gruppe im Hämoglobin durch resonante Ramanstreuung. Doctoral thesis, Bremen

Schweitzer-Stenner R, Dreybrodt W (1985) Excitation profiles and depolarization ratios of some prominent Raman lines in oxyhaemoglobin and ferrocytochrome *c* in the preresonant and resonant region of the *Q*-band. J Raman Spectrosc 16:111–123

Schweitzer-Stenner R, Dreybrodt W (1989) An extended MWC-model expressed in terms of the Herzyfeld-Stanley formalism applied to oxygen and carbonmonoxide binding curves of hemoglobin trout IV. Biophys J 55:691–701

Schweitzer-Stenner R, Dreybrodt W, el Naggar S (1984a) Investigation of pH-induced symmetry distortions of the prosthetic group in deoxyhemoglobin by resonance Raman scattering. Biophys Struct Mech 10:241–256

Schweitzer-Stenner R, Dreybrodt W, Wedekind D, el Naggar S (1984b) Investigation of pH-induced symmetry distortions of the prosthetic group in oxyhemoglobin by resonance Raman scattering. Eur Biophys J 11:61–76

Schweitzer-Stenner R, Wedekind D, Dreybrodt W (1986) Correspondence of the pK-values of oxyHb-titration states detected by resonance Raman scattering to kinetic data of ligand dissociation and association. Biophys J 49:1077–1088

Schweitzer-Stenner R, Wedekind D, Dreybrodt W (1989) Allosteric transitions in oxyHb trout IV detected by resonance Raman spectroscopy. Biophys J 55:703–705

Shaanan B (1983) Structure of human oxyhemoglobin at 2:1 Å resolution. J Mol Biol 171:31–59

Shih Tb, Jones RT, Bonaventura J, Bonaventura C, Schneider RG (1984) Involvement of His HC3(146)β in the Bohr effect of human hemoglobin. Studies of native and N-ethylmaleimido-treated hemoglobin A and hemoglobin Cowntown (β146 His → Leu). J Biol Chem 259:967–974

Simon SR, Arndt DJ, Konigsberg WH (1971) Structure and functional properties of chemically modified horse hemoglobin. J Mol Biol 58:69–77

Warshel A (1977) Energy-structure correlation in metalloporphyrins and the control of oxygen binding by hemoglobin. Proc Natl Acad Sci USA 74:1789–1793

Wedekind D, Schweitzer-Stenner R, Dreybrodt W (1985) Heme-apoprotein interaction in the modified oxyhemoglobin-bis-(N-maleimidomethyl) ether and in oxyhemoglobin at high Cl^--concentration detected by resonance Raman scattering. Biochim Biophys Acta 830:224–232

Wedekind D, Brunzel U, Schweitzer-Stenner R, Dreybrodt W (1986) Correlation of pH-dependent resonance Raman and optical absorption data reflecting heme-apoprotein interaction in oxyhaemoglobin. J Mol Struct 143:457–460